Civil Engineering and Applied Solutions

Research Article

journal homepage: ceas.journals.umz.ac.ir

CEAS Civil Engineering and Applied Solutions

Data-Driven Predictive Formulation for FRP-Confined Circular Concrete Columns

Sajjad Shayanfar [a], Meysam Ghasemi Naghibdehi [a], Javad Shayanfar [b*]

[a] *Department of Civil Engineering, Qaemshahr Branch, Islamic Azad University, Qaemshahr, Iran*
[b] *Department of Civil Engineering, University of Minho, Azurém, Guimarães 4800-058, Portugal*

ARTICLE INFO

Article history:

Received 10 December 2025

Revised 06 January 2026

Accepted 29 January 2026

Available online 01 January 2027

Keywords:

FRP confinement

Compressive strength

Predictive model

Design-oriented model

Confined concrete

ABSTRACT

This study presents a new design-oriented, regression-based model for predicting the ultimate compressive strength of circular concrete columns confined with fiber-reinforced polymer (FRP) jackets. The model is grounded in fundamental confinement mechanics and accounts for key parameters, including FRP elastic modulus, ultimate tensile strain, confinement stiffness, unconfined concrete strength, and column diameter. A comprehensive and rigorously filtered experimental database comprising 1,376 FRP-confined circular concrete specimens was assembled, covering concrete strengths from 6.6 to 204 MPa and FRP types including CFRP, GFRP, BFRP, and AFRP. A carefully curated experimental database of 1,376 circular FRP-confined specimens was assembled, covering a broad spectrum of concrete strengths and FRP types. Regression analysis was used to calibrate the model, and a dimension-based correction factor was incorporated to capture the influence of cross-sectional geometry. The resulting formulation demonstrates robust predictive capability and general applicability across diverse concrete strengths and column geometries, providing a reliable tool for practical engineering design. Parametric studies further illustrate how confinement efficiency varies with concrete strength and FRP properties, offering guidance for optimizing FRP confinement in practice.

How to cite this article: Shayanfar, S., Ghasemi Naghibdehi, M., Shayanfar, J. Data-Driven Predictive Formulation for FRP-Confined Circular Concrete Columns. Civil Engineering and Applied Solutions. 2027; 3(1): 25–36. doi:10.22080/ceas.2026.30751.1060.

1. Introduction

In recent years, fiber-reinforced polymer (FRP) composites have emerged as a highly effective and widely adopted method for the seismic retrofitting and performance enhancement of reinforced concrete (RC) columns originally designed without seismic considerations [1-7]. The application of externally bonded FRP jackets provides significant improvements in both axial load-carrying capacity and lateral dilation resistance of concrete columns under compressive loading by constraining the transverse expansion of the concrete core. This confinement mechanism not only increases the ultimate compressive strength but also enhances ductility and energy dissipation under seismic actions [8-11]. Despite the extensive practical implementation of FRP confinement, the development of accurate constitutive models that predict the combined effects of FRP-induced confinement on the axial and lateral responses of concrete remains an active area of research. These models aim to capture the nonlinear interaction between concrete core behavior, FRP stiffness and thickness, number of layers, and the influence of concrete strength, providing reliable tools for both design and assessment of confined columns [12-16].

Under axial compressive loading, FRP-confined concrete columns with circular cross-sections may exhibit strain-softening behavior, which is influenced primarily by (i) the stiffness of the FRP confinement and (ii) the concrete strength class [17-21]. In general, low-strength concrete (LSC) and normal-strength concrete (NSC) columns that are adequately confined by an FRP jacket tend to demonstrate a full hardening stress-strain response accompanied by distributed micro-cracking. However, as the imposed confinement stiffness decreases, LSC and NSC columns begin to display post-peak strain-softening behavior after the transition

* Corresponding author.
E-mail addresses: arch3d.ir@gmail.com (J. Shayanfar).

https://doi.org/10.22080/ceas.2026.30751.1060
ISSN: 3092-7749/

zone, similar to unconfined concrete (UC) columns when the confinement stiffness is very low. Experimental investigations into high-strength concrete (HSC) and ultra-high-strength concrete (UHSC) columns confined with FRP jackets reveal behaviors that differ notably from NSC columns, highlighting several key phenomena. Ozbakkaloglu and Akin [17] demonstrated that the confinement-induced enhancements in compressive strength and strain ductility decrease significantly as the concrete strength increases. This results in a delayed development of axial strain and stress relative to the confining FRP strain and stress. While increasing FRP confinement stiffness generally improves the response of confined concrete, the degree of improvement is strongly dependent on the concrete strength: NSC columns benefit more from increased stiffness than HSC or UHSC columns [22-26]. Unlike NSC columns, FRP-confined HSC and UHSC columns tend to exhibit post-peak strain-softening behavior following the transition zone due to this confinement lag, which often manifests as localized macro-cracks [27]. By increasing the FRP confinement stiffness, the lateral restraint can sufficiently counteract the expansive tendencies of the concrete, mitigating post-peak strength degradation. In such cases, the column may exhibit either a strain post-peak softening-hardening response or a fully hardening stress-strain behavior [19, 28-33].

For simulating the mechanical behavior of FRP-confined concrete under concentric compressive loading, numerous constitutive models have been developed [8, 24, 25, 34-40] , which can generally be classified into two categories: analysis-oriented and design-oriented models. Analysis-oriented models predict the stress–strain behavior of FRP-confined concrete using incremental dilation-based approaches (e.g., [41-48]). Axial strain is first computed from a given FRP hoop strain (i.e., confinement pressure) using a dilation model, and the corresponding axial stress is then determined via a stress–strain relation developed for actively confined concrete. Although these models assume that passively and actively confined concrete behave similarly at a given hoop strain, differences are accounted for through the failure surface function, known as the confinement path effect. Design-oriented models, in contrast, provide simplified closed-form expressions for the stress–strain response of FRP-confined concrete columns, with model parameters calibrated against experimental data [8, 49-51]. For instance, Lam and Teng [8] proposed a parabolic–linear stress–strain relationship for FRP-confined NSC columns, predicting ultimate axial stress and strain based on the actual FRP hoop strain at rupture. However, this model does not account for a descending branch in the stress–strain curve. Subsequent guidelines, such as ACI [52] and fib [53], adopted Lam and Teng's recommendations with modifications, including confinement pressure thresholds below which strength enhancement is neglected and updated formulations for calculating FRP hoop strain. Teng et al. [49] refined Lam and Teng's model by updating the ultimate strength and strain expressions using numerical results from Jiang and Teng [41] and an extended experimental database. By introducing a confinement stiffness threshold, this refined model can capture either hardening or softening behavior in the stress–strain curve. Lim and Ozbakkaloglu [54] formulated predictive expressions for ultimate axial strength and strain of FRP-confined NSC and HSC columns based on a comprehensive test dataset, though a full stress–strain model was not provided. Fallah Pour et al. [51] proposed a simplified design-oriented model using a large database of NSC and HSC columns, providing closed-form expressions for stress and strain at ultimate and transition stages. Despite the significant progress in developing stress–strain models for FRP-confined concrete, most existing models are constrained to specific concrete strength classes (e.g., NSC or HSC), limiting their general applicability across the full spectrum of concrete strengths.

Most existing models were calibrated using relatively limited experimental databases, often encompassing a narrow range of parameters such as confinement stiffness, concrete strength, and specimen geometry, and featuring low data density [55]. Consequently, their predictive reliability becomes questionable when applied to broader datasets that cover a wider spectrum of concrete strengths, FRP properties, and column geometries. The accuracy and reliability of regression-based predictive formulations for FRP-confined concrete are fundamentally dependent on the quality, diversity, and comprehensiveness of the experimental database used for model calibration [56]. A high-quality database must encompass a wide range of key parameters, including concrete compressive strength, FRP mechanical properties, column geometry, and confinement configurations, to fully capture their individual and interactive effects on structural behavior. Inadequate, sparse, or biased datasets can lead to models that are valid only within limited parameter ranges, thereby reducing their generalizability and predictive robustness. Moreover, a comprehensive and statistically representative database enables rigorous regression analysis, allowing the derivation of model coefficients that accurately reflect both the mean response and variability in experimental outcomes. This ensures that the resulting predictive formulation can reliably estimate ultimate axial strength, strain capacity, and stress–strain behavior under various confinement conditions, while also providing a sound basis for uncertainty quantification in practical design applications.

In this study, a new design-oriented constitutive model is developed to predict the ultimate compressive strength of circular concrete columns confined with FRP jackets. The model is grounded in the fundamental mechanics of confinement, explicitly incorporating the effects of FRP material properties (elastic modulus and ultimate tensile strain), confinement stiffness, unconfined concrete strength, and, critically, the cross-sectional size through a dimension-based correction factor. Leveraging a large, high-quality experimental database of 1,376 specimens that spans low- to ultra-high-strength concrete and a wide array of FRP types and configurations, the model is calibrated using robust regression techniques. Unlike many existing formulations that are limited to specific concrete strength ranges or neglect geometric scale effects, the proposed model offers a unified, accurate, and broadly applicable prediction framework. Its development addresses a critical gap in current practice by reconciling mechanistic principles with empirical evidence across the full spectrum of practical FRP confinement scenarios, thereby enhancing the reliability of strength assessments in both retrofit and new-design applications. It should be emphasized that the contribution of this study extends beyond empirical recalibration using an expanded dataset. A key innovation lies in the explicit recognition and quantification of geometric scale effects, specifically, the reduction in confinement effectiveness with increasing column diameter, which has been historically overlooked or implicitly absorbed into empirical coefficients in existing models. This work introduces a mechanistically informed, dimension-based correction factor that directly accounts for this phenomenon. Furthermore, the proposed formulation achieves true unification across an unprecedented concrete strength range (6.6–204 MPa) through a single, continuous expression

governed by confinement stiffness, rather than relying on piecewise functions or strength-class-specific calibrations. These features represent a conceptual advance in transitioning from purely empirical correlations toward physics-informed, data-driven modeling of FRP-confined concrete.

2. Compressive behavior of concrete confined with FRP jackets

The fundamental principle governing the confinement mechanism of FRP-jacketed concrete is as follows: when a certain level of axial strain (ε_c) is applied to the concrete, a corresponding radial (lateral) strain $\varepsilon_l = \nu \times \varepsilon_c$ develops according to Poisson's ratio (ν) [57]. Since the radial strain is equal to the hoop strain ($\varepsilon_h = \varepsilon_l$) [34], the radial expansion of the concrete transforms into hoop strain around the concrete core. Assuming full compatibility between the concrete and the FRP sheets, this hoop strain is subsequently transferred to the FRP jacket as tensile strain ($\varepsilon_{h,f} = \varepsilon_h = \varepsilon_l = \nu \times \varepsilon_c$). Therefore, to produce a given level of axial strain in the concrete, an equivalent level of tensile strain (and consequently tensile stress (f_f)) must be induced in the FRP sheets. In other words, under axial loading, confined concrete requires a higher axial compressive stress (f_c) than unconfined concrete to reach the same axial and lateral strain levels that mobilize the desired tensile response in the FRP. The tensile stress developed in the FRP is then transferred back to the concrete in the form of a confining pressure ($f_{l,f}$), which restrains the lateral expansion of the concrete column. Therefore, by using FRP sheets, it is possible to restrain the axial and lateral deformation of concrete, which would otherwise lead to cracking and stiffness degradation. This restraining action is referred to as the confinement mechanism of concrete. The force equilibrium in a concrete column section with width b and height L, between the tensile force developed in the FRP and the confining pressure applied to the concrete, can be expressed as:

$$f_{l,f} \times Lb = 2f_f \times Ln_f t_f \tag{1}$$

where n_f and t_f denote the number of FRP layers and the thickness of each FRP layer, respectively. By simplifying the above relation, the confining pressure $f_{l,f}$ can be computed as follows:

$$f_{l,f} = 2\frac{n_f t_f f_f}{b} \tag{2}$$

By considering that the tensile stress developed in the FRP sheets (f_f) is equal to the product of the elastic modulus (E_f) and the tensile strain in the FRP jacket ($\varepsilon_{h,f}$), the above expression can be rewritten as follows:

$$f_{l,f} = 2\frac{n_f t_f E_f \varepsilon_{h,f}}{b} \tag{3}$$

Based on experimental studies conducted on concrete columns confined with FRP, it has been shown that at the ultimate state corresponding to the maximum compressive strength (f_{cc}), the hoop rupture strain in the FRP ($\varepsilon_{h,rup}$) is smaller than the ultimate tensile strain of the FRP (ε_{fu}) obtained from direct tensile testing. For example, ACI [52] recommends a ratio of 0.55 between $\varepsilon_{h,rup}$, and ε_{fu}. Therefore, by assuming a constant ratio η between these two parameters, $\varepsilon_{h,rup}$ can be expressed as:

$$\varepsilon_{h,rup} = \eta\varepsilon_{fu} \tag{4}$$

By substituting Eq. 4 into Eq. 3, the ultimate stress developed in the FRP corresponding to the maximum confining pressure can be written as:

$$f_{l,f,u} = 2\frac{n_f t_f E_f \varepsilon_{h,rup}}{b} = 2\eta\frac{n_f t_f E_f \varepsilon_{fu}}{b} \tag{5}$$

The lateral confinement stiffness provided by the FRP is defined as the ratio of the confining pressure ($f_{l,f}$) to the hoop strain developed in the FRP ($\varepsilon_{h,f}$), and can be expressed as:

$$K_L = \frac{f_{l,f}}{\varepsilon_{h,f}} = \frac{f_{l,f,u}}{\varepsilon_{h,rup}} = 2\frac{n_f t_f E_f}{b} \tag{6}$$

Therefore, Eq. 5 can be simplified as follows:

$$f_{l,f,u} = \eta K_L \varepsilon_{fu} \tag{7}$$

On the other hand, the ultimate compressive strength of FRP-confined concrete columns is generally expressed as:

$$f_{cc} = f_{c0} + \beta_1 \left(f_{l,f,u}\right)^{\beta_2} \tag{8}$$

where β_1 and β_2 are constant coefficients obtained through regression analysis. By normalizing the above equation with respect to the compressive strength of unconfined concrete (f_{c0}), the following relation is obtained:

$$\frac{f_{cc}}{f_{c0}} = 1 + \beta_1 \left(\frac{f_{l,f,u}}{f_{c0}}\right)^{\beta_3} \tag{9}$$

where β_3 is another constant determined from regression analysis. Therefore, by substituting Eq. 7 into Eq. 9, we obtain:

$$\frac{f_{cc}}{f_{c0}} = 1 + \beta_1 \left(\frac{\eta K_L \varepsilon_{fu}}{f_{c0}}\right)^{\beta_3} = 1 + \beta_1 \eta^{\beta_3} {K_L}^{\beta_3} {\varepsilon_{fu}}^{\beta_3} {f_{c0}}^{-\beta_3} \tag{10}$$

Considering that the expression $\beta_1 \eta^{\beta_3}$ is a constant value, it may be replaced by a new constant coefficient β_4. Therefore, Eq. 10

can be rewritten as:

$$\frac{f_{cc}}{f_{c0}} = 1 + \beta_4 {K_L}^{\beta_3} {\varepsilon_{fu}}^{\beta_3} {f_{c0}}^{-\beta_3} \quad (11)$$

As can be observed, the above relation is a function of K_L, ε_{fu}, and f_{c0}. To obtain a suitable form for regression analysis, the structure of the equation is modified as follows:

$$\frac{f_{cc}}{f_{c0}} = \beta_5 {K_L}^{\beta_6} {\varepsilon_{fu}}^{\beta_7} {f_{c0}}^{\beta_8} \geq 1 \quad (12)$$

where β_5 to β_8 are constant coefficients obtained from regression analysis, which will be presented later. It is important to note that although the structure of Eq. 11 is modified, the key parameters (K_L, ε_{fu}, and f_{c0}) are still included in Eq. 12. Furthermore, for the case where the confinement stiffness (K_L) approaches zero (representing unconfined concrete), the result of both equations becomes equal to unity ($\frac{f_{cc}}{f_{c0}} = 1$).

3. Test database of FRP-confined concrete columns

To calibrate the proposed formula in Eq. 12 through regression analysis, a comprehensive database of experimental results from FRP-confined concrete columns is required. This database also enables the evaluation of the reliability of the proposed formula as well as existing models in the literature.

In this paper, an extensive database has been compiled from experimental specimens tested under axial compressive loading. To ensure a consistent and unified database of experimental results, the following criteria were applied:

1. Specimens containing conventional steel longitudinal or transverse reinforcement were excluded.
2. Specimens with partial confinement configurations were excluded.
3. Specimens confined using spiral wrapping were excluded.
4. Specimens exhibiting FRP debonding as the failure mode were excluded.
5. Specimens confined simultaneously with different types of FRP materials (hybrid confinement) were excluded.
6. Specimens subjected to eccentric axial loading were excluded.
7. Experimental results in which the ultimate compressive strength of the confined specimen (f_{cc}) was lower than that of the unconfined concrete (f_{c0}) were excluded (i.e., $f_{cc} < f_{c0}$).
8. Only specimens confined with CFRP, BFRP, AFRP, and GFRP (materials with linear tensile stress–strain behavior) were included.
9. Specimens confined with PEN- or PET-based fibers, which exhibit nonlinear tensile stress–strain behavior, were excluded.

Table 1 summarizes the statistical characteristics of 1,376 FRP-confined circular concrete column specimens compiled from various experimental studies. This database captures a wide range of parameters, reflecting differences in material properties, geometry, and FRP confinement characteristics, which is crucial for developing and calibrating predictive models. Concrete Strengths (f_{c0} and f_{cc}): The compressive strength of unconfined concrete (f_{c0}) spans from 6.6 MPa to 204 MPa, with a mean value of 48.5 MPa and a coefficient of variation (CoV) of 0.71. This indicates that the database includes low- to high-strength concrete. The compressive strength of FRP-confined concrete (f_{cc}) ranges from 17.8 MPa to 381 MPa, with a mean of 87.4 MPa and a CoV of 0.58, reflecting the strength enhancement due to FRP confinement. The confinement effect, measured as the ratio f_{cc} / f_{c0}, varies between 1.05 and 6.9, with a mean of 2.03 and a CoV of 0.41, showing substantial variability in the confinement efficiency across specimens. Specimen Geometry (L and b): The column heights (L) range from 100 mm to 915 mm, with a mean of 301 mm (CoV = 0.37). The diameters of circular sections (b) vary from 50 mm to 305 mm, with a mean of 144 mm (CoV = 0.31). These variations capture both small-scale laboratory specimens and larger-scale columns, ensuring that the database can support models applicable to a wide range of practical scenarios. FRP Material Properties (E_f, $n_f \times t_f$, ε_{fu}): The FRP elastic modulus (E_f) ranges from 13.6 GPa to 657 GPa, with a mean of 190 GPa (CoV = 0.52), representing different FRP types including glass, carbon, basalt, and aramid fibers. The total thickness of the FRP layers ($n_f \times t_f$) spans 0.057 mm to 5.1 mm, with a mean of 0.581 mm (CoV = 1.19), showing a wide range of confinement intensities. The ultimate tensile strain of the FRP (ε_{fu}) varies from 0.004 to 0.037, with a mean of 0.018 (CoV = 0.32), reflecting the diverse ductility characteristics of the FRP materials used. Overall, this database is comprehensive, covering a broad spectrum of concrete strengths, column geometries, and FRP confinement properties. The statistical distributions of the key parameters (strength, geometry, and FRP characteristics) demonstrate significant variability, which is essential for developing reliable regression models and for evaluating the performance of FRP-confined concrete under axial loading. The large sample size (1,376 specimens) ensures robust statistical analysis and model calibration.

The dataset was screened for outliers using standardized residuals and leverage diagnostics. Observations with standardized residuals greater than ±3 were identified as extreme. Leverage statistics were used to evaluate the influence of predictor values: observations with leverage below 0.2 were considered non-influential, those between 0.2 and 0.5 were monitored but generally retained unless accompanied by near-extreme residuals, and values exceeding 0.5 were subjected to detailed scrutiny for possible

measurement errors or undue influence on the model.

Table 1. Details of the database of FRP-confined concrete columns.

Section shape	Number of data	Statistical index	f_{c0} (MPa)	f_{cc} (MPa)	f_{cc}/f_{c0}	L (mm)	b (mm)	E_f (GPa)	$n_f t_f$ (mm)	ε_{fu}
Circle	1376	Minimum	6.6	17.8	1.05	100	50	13.6	0.057	0.004
		Maximum	204	381	6.9	915	305	657	5.1	0.037
		Mean	48.5	87.4	2.03	301	144	190	0.581	0.018
		CoV	0.71	0.58	0.41	0.37	0.31	0.52	1.19	0.32

Data points identified by either diagnostic were excluded only when they were determined to meaningfully distort the regression results, thereby supporting the robustness and reliability of the analysis.

4. Proposed formula for circular FRP-confined concrete columns

In the present study, the experimental data from the database were used to determine the coefficients of Eq. 12. Based on 1376 experimental specimens of circular concrete columns, a relationship between the ratio of the maximum compressive strength of confined concrete (f_{cc}/f_{c0}) and the key parameters ε_{fu}, K_L, and f_{c0} is proposed as follows:

$$\frac{f_{cc}}{f_{c0}} = 3.1{K_L}^{0.36}{\varepsilon_{fu}}^{0.23}{f_{c0}}^{-0.55} \geq 1 \quad (13)$$

The predictive capability of the proposed formula is illustrated in Fig. 1. As can be observed, based on statistical indices such as the mean, coefficient of variation (CoV), mean absolute percentage error (MAPE), and the coefficient of determination (R^2), Eq. 13 provides satisfactory accuracy for predicting the ultimate compressive strength of circular FRP-confined concrete columns.

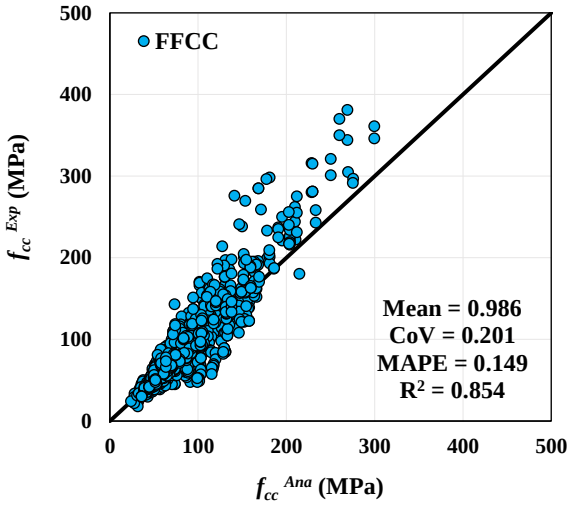

Fig. 1. Comparison of the predicted ultimate compressive strength from the proposed model based on 1376 experimental circular FRP-confined concrete column specimens.

It should be noted that in Eq. 13, the effects of section dimensions were not considered in the regression analysis. Experimental studies [11–13] have shown that, as the column cross-sectional dimensions increase, the effectiveness of the FRP confinement decreases. Therefore, to account for the influence of this parameter, an error analysis of the proposed model must be conducted. Fig. 2a shows the relationship between the analytical-to-experimental ratio ($Y_1 = f_{cc}^{Ana} / f_{cc}^{Exp}$) and the section aspect factor ($R_b = b / 150$). As observed, there is a clear dependency between the error (Y_1) and R_b, indicating the necessity of considering the effects of section dimensions. For specimens with low RbR_bRb, the proposed model tends to provide slightly conservative predictions, whereas for specimens with high R_b, the model also produces conservative estimates. Using regression analysis, the relationship between the prediction error (Y_1) and the section aspect factor (R_b) was obtained as follows:

$$Y_1 = \frac{{f_{cc}}^{Ana}}{{f_{cc}}^{Exp}} = {R_b}^{0.14} \quad (14)$$

By substituting Eq. 14 into Eq. 13, the ultimate compressive strength of the confined concrete (f_{cc}) can be determined.

$$\frac{f_{cc}}{f_{c0}} = \frac{3.1{K_L}^{0.36}{\varepsilon_{fu}}^{0.23}{f_{c0}}^{-0.55}}{{R_b}^{0.14}} \geq 1 \quad (15)$$

The above equation can also be expressed in the following form:

$$\frac{f_{cc}}{f_{c0}} = 3.1{K_L}^{0.36}{\varepsilon_{fu}}^{0.23}{f_{c0}}^{-0.55}{R_b}^{-0.14} \geq 1 \quad (16)$$

Based on the statistical indicators presented in Fig. 2b, Eq. 16 demonstrates high accuracy in predicting the ultimate compressive strength of circular concrete columns confined with FRP jackets. The statistical evaluation includes metrics such as the mean ratio, coefficient of variation (CoV), mean absolute percentage error (MAPE), and the coefficient of determination (R^2), all of which indicate that the proposed model closely matches the experimental results. Furthermore, by comparing the statistical indices obtained for Eq. 13 and Eq. 16, it can be concluded that incorporating the effects of cross-sectional dimensions significantly improves the predictive performance of the model. Specifically, while Eq. 13 tends to exhibit systematic deviations for specimens with high or low aspect ratios (R_b), Eq. 16 accounts for these geometric effects, resulting in reduced bias and error variability. Fig. 2c illustrates the relationship between the prediction error of Eq. 16 and the section aspect factor (R_b). As observed, after applying the correction factor $R_b^{-0.14}$ in the proposed equation, the prediction error, defined as $Y_2 = f_{cc}^{Ana} / f_{cc}^{Exp} - 1$, exhibits no significant correlation with R_b. This indicates that the proposed formula successfully captures the influence of cross-sectional dimensions on the confinement effectiveness, leading to a more robust and dimension-independent predictive model for circular FRP-confined concrete columns.

The proposed formulation is developed specifically for circular FRP-confined concrete columns under axial compressive loading using linear-elastic FRP materials (CFRP, BFRP, AFRP, GFRP) with full and uniform confinement. Specimens with conventional steel reinforcement, partial confinement, spiral wrapping, hybrid FRP types, eccentric loading, nonlinear FRP materials (e.g., PEN or PET-based fibers), or cases where $f_{cc}<f_{c0}$ were excluded from the database. Therefore, the model is not directly applicable to columns outside these conditions. Users should exercise caution when applying the formulation to partially confined columns, internally reinforced columns, eccentrically loaded specimens, columns with nonlinear FRP, or large-scale structural columns, as the predictive accuracy under these conditions has not been validated.

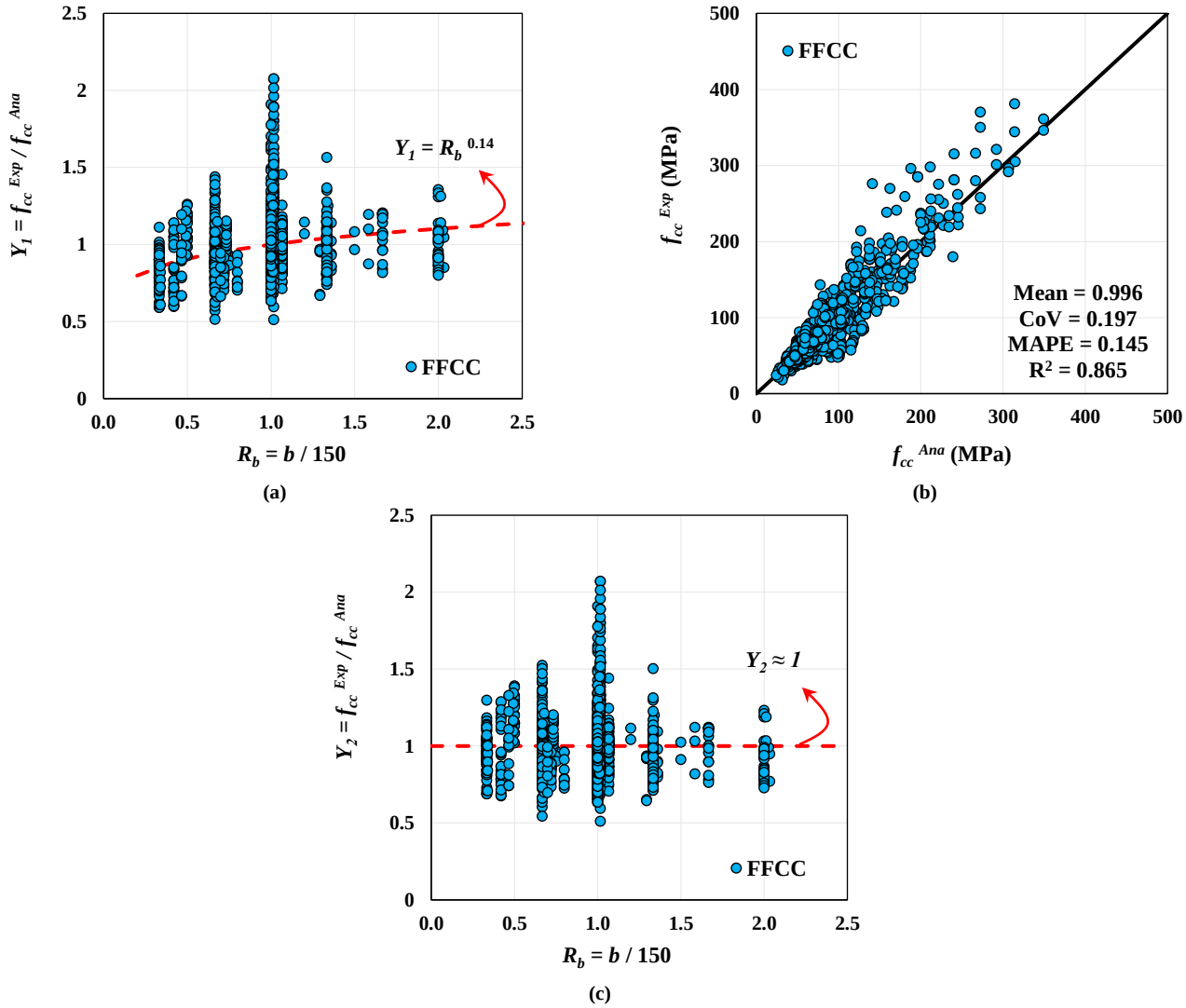

Fig. 2. Evaluation of the predicted ultimate compressive strength of FRP-confined circular columns using the proposed model, based on 1376 experimental specimens.

In this section, a parametric study was conducted to investigate the influence of key parameters on the ultimate compressive strength of FRP-confined concrete columns. For this purpose, a circular concrete column with a smaller dimension of b = 250 mm was considered. The mechanical properties of the FRP were assumed as follows: elastic modulus E_f = 240GPa, nominal thickness t_f = 0.17mm, and ultimate tensile strain ε_{fu}=0.017. Fig. 3 illustrates the effects of FRP confinement stiffness (K_L) and the compressive strength of unconfined concrete (f_{c0}) on the confinement effectiveness for circular concrete columns. In this figure, the relationship between the compressive strength of the FRP-confined column (f_{cc}) and the unconfined concrete strength (f_{c0}) is plotted for different levels of lateral confinement stiffness (K_L). As shown, increasing the unconfined concrete strength (f_{c0}) has a negative effect on the

compressive strength of the confined column (f_{cc}), indicating that higher-strength concrete benefits less from FRP confinement. For instance, when K_L = 321MPa, no significant increase in the column strength is observed for unconfined concrete strengths exceeding 50 MPa. However, as the lateral confinement stiffness (K_L) increases, the negative influence of f_{c0} is substantially reduced, and a pronounced enhancement in the ultimate compressive strength of the column is achieved. This underscores the pivotal role of K_L in controlling the lateral restraint and hoop stress development in FRP-confined concrete columns. Higher K_L values lead to more effective engagement of the confinement mechanism, mitigating the reduction in lateral dilation observed in high-strength concrete, which inherently exhibits lower volumetric strain under axial loading. Consequently, the stiffness of the FRP jacket not only enhances the ultimate compressive strength (f_{cc}) but also improves ductility and delays premature failure modes such as concrete crushing or FRP rupture. These effects highlight that accurate specification of FRP material properties, layer thickness, and number of layers is essential for optimizing the performance of confined columns, particularly when designing for high-strength concrete applications where confinement efficiency is otherwise reduced.

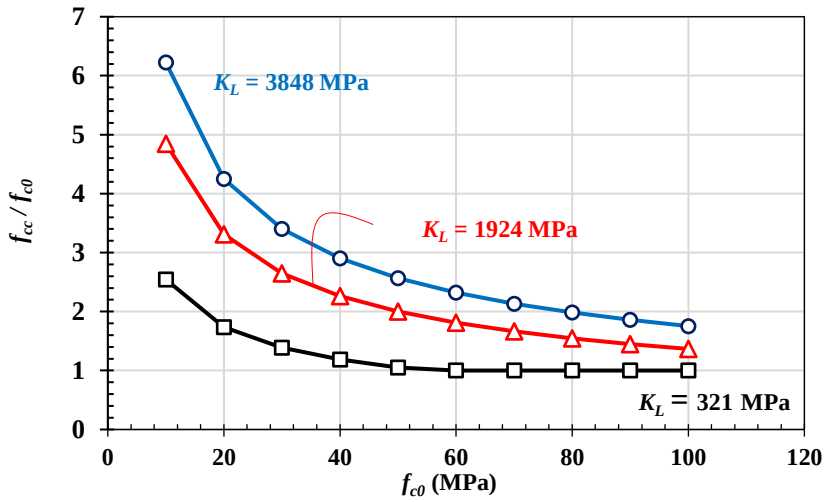

Fig. 3. Investigation of the effects of FRP confinement stiffness and unconfined concrete compressive strength on the ultimate strength of circular concrete columns.

5. Comparison of the proposed model with existing models

Fig. 4 and Table 2 compare the experimental results with the predictions obtained from existing analytical models and the proposed model. In both the figure and the table, the statistical indices presented include the mean absolute percentage error (MAPE), mean squared error (MSE), coefficient of variation (CoV), mean value (MV), and coefficient of determination (R^2).

$$MV = \frac{1}{n}\sum_{1}^{n}\frac{T_i}{E_i} \tag{17}$$

$$CoV = \frac{SD}{MV} \tag{18}$$

$$MSE = \frac{1}{n}\sum_{1}^{n}(T_i - E_i)^2 \tag{19}$$

$$MAPE = \frac{1}{n}\sum_{1}^{n}\left|1 - \frac{T_i}{E_i}\right| \tag{20}$$

$$R^2 = \left(\frac{\sum_{1}^{n}[(T_i - \bar{T}_i)(E_i - \bar{E}_i)]}{\sqrt{\sum_{1}^{n}[(T_i - \bar{T}_i)^2(E_i - \bar{E}_i)^2]}}\right)^2 \tag{21}$$

where T_i and E_i are $\frac{f_{cc}}{f_{c0}}$ obtained analytically and experimentally, respectively. SD is standard deviation; n is the number of data; $\bar{T}$and $\bar{E}_i$represents the mean values of the analytical and experimental predictions, respectively.

These indices provide a comprehensive evaluation of the predictive accuracy of each model relative to the experimental data. As can be observed, based on MV and CoV, the model proposed by Fib [17] exhibits the best performance among the existing models, with MV = 0.892 and CoV = 0.226. However, this model still tends to slightly underestimate the experimental values,

producing somewhat conservative predictions. In terms of MSE and MAPE, the fib [17] model also achieves the lowest values among the existing models, confirming its superior predictive performance. The coefficient of determination (R^2) for both the fib [17] model and Guo et al. [51] is 0.820, indicating a strong correlation with the experimental data. Overall, the fib [17] model performs best among the existing models for predicting the ultimate compressive strength of circular FRP-confined concrete columns. On the other hand, the model proposed by Cao et al. [50] shows the weakest performance among the existing models, providing non-conservative predictions with high scatter. When comparing the proposed model with the fib [17] model, it is evident that the proposed model outperforms all existing models across all statistical indices. This enhanced performance is attributed to the inclusion of critical parameters such as FRP tensile strain, confinement stiffness, unconfined concrete strength, and geometric effects, which are grounded in the mechanical behavior of FRP-confined concrete. The results confirm that the proposed model provides a robust, statistically significant improvement over existing formulations and captures the underlying confinement mechanics more accurately.

Table 2. Comparison of existing analytical models' predictions of ultimate strength for circular FRP-confined concrete columns.

Analytical Model	R2	MAPE	MSE	CoV	MV
ACI [52]	0.812	0.189	0.375	0.279	0.938
fib [53]	0.82	0.185	0.343	0.226	0.892
Cao et al. [47]	0.782	0.257	1.03	0.313	1.219
Wei and Wu [50]	0.812	0.189	0.426	0.282	1.078
Guo et al. [46]	0.82	0.266	0.628	0.252	0.77
Proposed Model	0.865	0.145	0.202	0.197	0.996

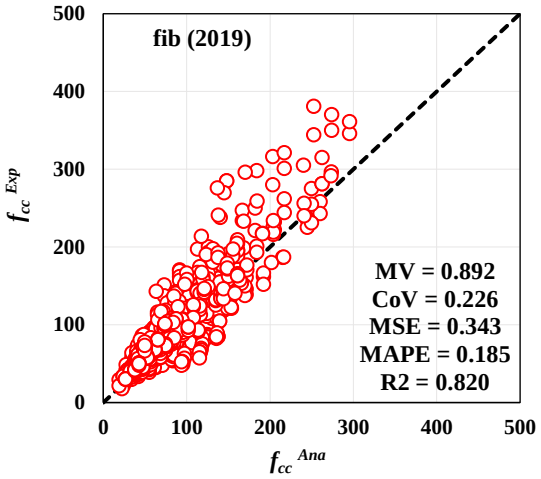

(a)

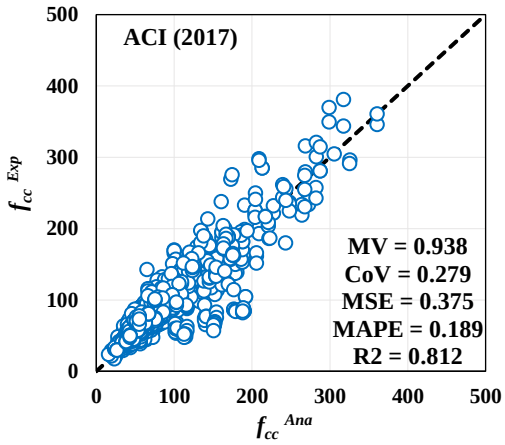

(b)

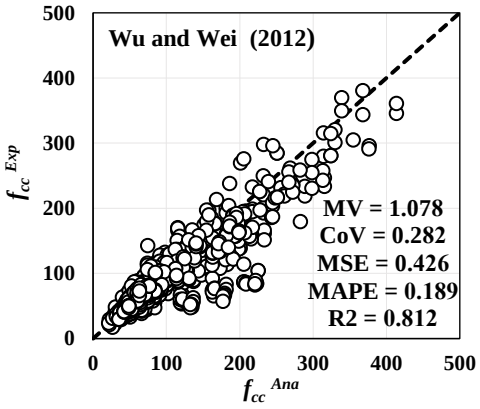

(c)

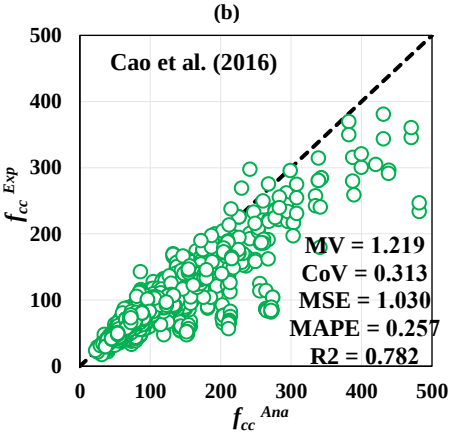

(d)

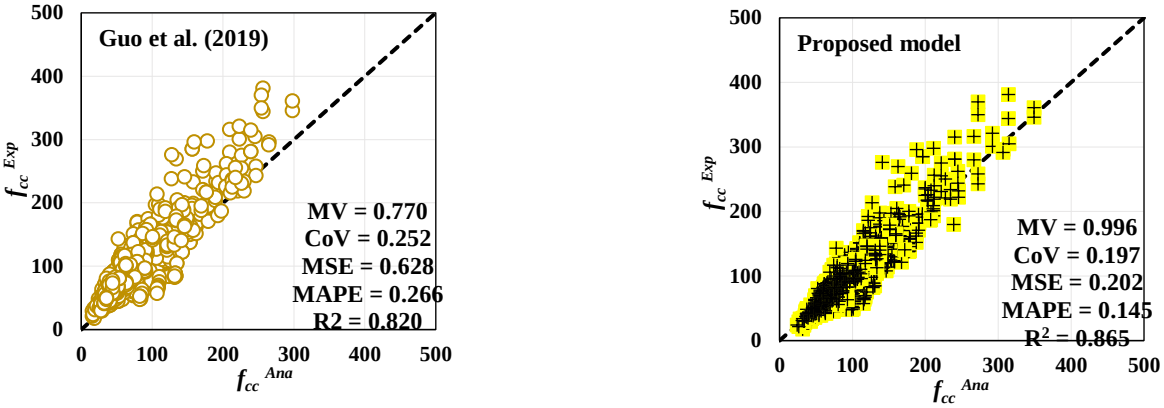

Fig. 4. Comparison of experimental results and predictions from analytical models based on 1376 circular concrete column specimens.

6. Numerical example

In this section, numerical examples are presented to demonstrate the application of the proposed formula for predicting the ultimate compressive strength of FRP-confined concrete columns under different confinement scenarios. Consider a circular concrete column with a diameter of b = 250 mm, confined with three layers of CFRP (n_f = 3). The mechanical properties of the CFRP are assumed as follows: E_f = 240 GPa, t_f = 0.17 mm, and ε_{fu} = 0.017. The unconfined concrete compressive strength is assumed to be f_{c0} = 25 MPa. The goal is to calculate the compressive strength of the FRP-confined column (f_{cc}).

Step 1: Calculation of confinement stiffness (K_L)

$$K_L = 2\frac{n_f t_f E_f}{b} = 2\frac{3 \times 0.17 \times 240000}{250} = 979.2 \text{ MPa}$$

Step 2: Calculation of ultimate compressive strength (f_{cc})

$$\frac{f_{cc}}{f_{c0}} = 3.1{K_L}^{0.36}{\varepsilon_{fu}}^{0.23}{f_{c0}}^{-0.55}{R_b}^{-0.14} \geq 1$$

$$\frac{f_{cc}}{f_{c0}} = 3.1(979.2)^{0.36}(0.017)^{0.23}(25)^{-0.55}\left(\frac{250}{150}\right)^{-0.14} = 2.30 \geq 1$$

$$\rightarrow f_{cc} = 2.30 \times f_{c0} = 2.30 \times 25 = 57.4 \text{ MPa}$$

Thus, the predicted compressive strength of the CFRP-confined circular column is 57.4 MPa.

7. Conclusion

This study presents a comprehensive analytical and empirical investigation into the compressive behavior of concrete confined with fiber-reinforced polymer (FRP) jackets, with a focus on circular columns. Based on a mechanistic understanding of the confinement mechanism, where lateral expansion of concrete under axial loading induces hoop tensile stresses in the FRP jacket, which in turn generate confining pressure, the study derives a physically consistent formulation for predicting the ultimate compressive strength of FRP-confined concrete. A large and rigorously filtered experimental database comprising 1,376 circular FRP-confined concrete specimens was compiled to support model development and validation. The database spans a wide range of concrete strengths (6.6–204 MPa), column geometries (diameter: 50–305 mm; height: 100–915 mm), and FRP material properties (E_f: 13.6–657 GPa; ε_{fu}: 0.004–0.037), ensuring broad representativeness and enhancing the generalizability of the derived model. Through regression analysis, a new predictive formula (Eq. 13) was initially proposed, capturing the influence of FRP ultimate tensile strain, confinement stiffness, and unconfined concrete strength on the strength enhancement ratio (f_{cc}/f_{c0}). Subsequent error analysis revealed a systematic dependency of prediction accuracy on column diameter, consistent with known size effects in FRP confinement. To address this, a dimension-based correction factor tied to the section aspect ratio (R_b = b/150) was introduced, yielding a refined model (Eq. 16) that effectively eliminates geometric bias. The final proposed model demonstrates superior predictive performance compared to existing analytical approaches. Statistical evaluation shows a mean prediction ratio of 0.996, a low coefficient of variation (CoV = 0.197), a high coefficient of determination (R^2 = 0.865), and the lowest mean absolute percentage error (MAPE = 14.5%) among all considered models, including the widely used fib Model Code formulation. Importantly, the proposed predictive model is not merely a re-calibrated version of existing formulations but embodies two fundamental advances: (i) the explicit incorporation of a geometric scale effect via a dimension-based correction factor derived from systematic error analysis, and (ii) a unified, continuous functional form that consistently captures the interaction between FRP properties and concrete strength, from conventional to ultra-high-strength concrete, using confinement stiffness as a governing parameter. This approach moves beyond traditional empirical fitting by embedding physical insight into a data-driven framework, thereby offering both improved accuracy and broader generalizability. Parametric analysis further underscores two critical insights: (1) the effectiveness

of FRP confinement diminishes as unconfined concrete strength increases, and (2) this adverse effect can be mitigated by increasing the lateral confinement stiffness through higher FRP modulus, greater thickness, or additional layers. This highlights the importance of tailoring FRP jacket design to the concrete strength class to achieve optimal performance. In summary, the proposed model offers a robust, physically grounded, and empirically validated tool for predicting the ultimate compressive strength of circular FRP-confined concrete columns. Explicitly accounting for material properties, confinement mechanics, and geometric scale effects, it provides a significant advancement over existing formulations, supporting more accurate and reliable design of FRP-strengthened structural elements in practice. This enables engineers to optimize FRP jacket configurations for different concrete strength classes and reliably assess confinement effectiveness across a broad range of column geometries and FRP types. Additionally, the study advances existing knowledge by integrating mechanistic understanding with data-driven regression, introducing a unified functional form that captures the interaction between confinement stiffness and concrete strength, and explicitly addressing size effects through a dimension-based correction factor. These contributions collectively enhance both the scientific understanding of FRP confinement and the practical applicability of predictive models in structural engineering design.

Statements & Declarations

Author contributions

Sajjad Shayanfar: Investigation, Formal analysis, Data curation, Software, Writing - Original Draft.

Meysam Ghasemi Naghibdehi: Project administration, Resources, Writing - Review & Editing.

Javad Shayanfar: Conceptualization, Methodology, Software, Writing - Review & Editing.

Funding

The authors received no financial support for the research, authorship, and/or publication of this article.

Data availability

The data presented in this study will be available on request from the corresponding author.

Declarations

The authors declare no conflict of interest.

References

[1] Isleem Haytham, F., Wang, Z., Wang, D., Smith Scott, T. Monotonic and Cyclic Axial Compressive Behavior of CFRP-Confined Rectangular RC Columns. Journal of Composites for Construction, 2018; 22: 04018023. doi:10.1061/(ASCE)CC.1943-5614.0000860.

[2] Shayanfar, J., Bengar, H. A. A practical model for simulating nonlinear behaviour of FRP strengthened RC beam-column joints. Steel and Composite Structures, 2018; 27: 49–74. doi:10.12989/scs.2018.27.1.049.

[3] Nematzadeh, M., Mousavimehr, M., Shayanfar, J., Omidalizadeh, M. Eccentric compressive behavior of steel fiber-reinforced RC columns strengthened with CFRP wraps: Experimental investigation and analytical modeling. Engineering Structures, 2021; 226: 111389. doi:10.1016/j.engstruct.2020.111389.

[4] Shayanfar, J., Barros Joaquim, A. O., Abedi, M., Rezazadeh, M. Unified Compressive Strength and Strain Ductility Models for Fully and Partially FRP-Confined Circular, Square, and Rectangular Concrete Columns. Journal of Composites for Construction, 2023; 27: 04023053. doi:10.1061/JCCOF2.CCENG-4336.

[5] Shayanfar, J., Barros, J. A. O., Pereira, J. P. C. A versatile model with a design framework for axially-loaded FRP-confined concrete with/without a stress reduction-recovery behavior. Construction and Building Materials, 2024; 448: 138097. doi:10.1016/j.conbuildmat.2024.138097.

[6] Shayanfar, J., Pereira, J. P. C., Barros, J. A. O. Passive confinement scenarios for strengthening fire-damaged concrete columns: Experimental and analytical research. Structures, 2025; 73: 108375. doi:10.1016/j.istruc.2025.108375.

[7] Liu, P., Wang, X., He, W., Lu, D., Wu, Z., Zhang, X., Shao, Y. Axial compressive behavior of concrete columns strengthened with BFRP grids. Construction and Building Materials, 2025; 477: 141305. doi:10.1016/j.conbuildmat.2025.141305.

[8] Lam, L., Teng, J. G. Design-oriented stress–strain model for FRP-confined concrete. Construction and Building Materials, 2003; 17: 471–489. doi:10.1016/S0950-0618(03)00045-X.

[9] Fallah Pour, A., Nguyen, G. D., Vincent, T., Ozbakkaloglu, T. Investigation of the compressive behavior and failure modes of unconfined and FRP-confined concrete using digital image correlation. Composite Structures, 2020; 252: 112642. doi:10.1016/j.compstruct.2020.112642.

[10] Shayanfar, J., Barros, J. A. O., Rezazadeh, M. Cross-sectional and confining system unification on peak compressive strength of FRP confined concrete. Structural Concrete, 2023; 24: 1531–1545. doi:10.1002/suco.202200105.

[11] Shayanfar, J., Barros, J. A. O., Rezazadeh, M. Analytical model to predict axial stress-strain behavior of heat-damaged unreinforced concrete columns wrapped by FRP jacket. Engineering Structures, 2023; 289: 116244. doi:10.1016/j.engstruct.2023.116244.

[12] Liao, J., Zeng, J.-J., Zhuge, Y., Zheng, Y., Ma, G., Zhang, L. FRP-confined concrete columns with a stress reduction-recovery behavior: A state-of-the-art review, design recommendations and model assessments. Composite Structures, 2023; 321: 117313. doi:10.1016/j.compstruct.2023.117313.

[13] Shayanfar, J., Barros, J. A. O., Rezazadeh, M. Analysis-oriented model for partially FRP-and-steel-confined circular RC columns under compression. Engineering Structures, 2023; 276: 115330. doi:10.1016/j.engstruct.2022.115330.

[14] Shayanfar, J., Barros Joaquim, A. O., Rezazadeh, M. Stress–Strain Model for FRP-Confined Circular Concrete Columns Developing Structural Softening Behavior. Journal of Composites for Construction, 2024; 28: 04023065. doi:10.1061/JCCOF2.CCENG-4364.

[15] Shayanfar, J., Barros, J. A. O., Rezazadeh, M., Kafshgarkolaei, H. J. Enhancing the performance of heat-damaged rectangular RC columns using prestressed FRP confinement. Construction and Building Materials, 2025; 501: 144346. doi:10.1016/j.conbuildmat.2025.144346.

[16] Zeng, J.-J., Chen, J.-D., Liao, J., Chen, W.-J., Zhuge, Y., Liu, Y. Behavior of ultra-high performance concrete under true tri-axial compression. Construction and Building Materials, 2024; 411: 134450. doi:10.1016/j.conbuildmat.2023.134450.

[17] Ozbakkaloglu, T., Akin, E. Behavior of FRP-Confined Normal- and High-Strength Concrete under Cyclic Axial Compression. Journal of Composites for Construction, 2012; 16: 451–463. doi:10.1061/(ASCE)CC.1943-5614.0000273.

[18] Wei, Y., Wu, Y.-F. Experimental Study of Concrete Columns with Localized Failure. Journal of Composites for Construction, 2016; 20: 04016032. doi:10.1061/(ASCE)CC.1943-5614.0000686.

[19] Shan, B., Gui, F. C., Monti, G., Xiao, Y. Effectiveness of CFRP Confinement and Compressive Strength of Square Concrete Columns. Journal of Composites for Construction, 2019; 23: 04019043. doi:10.1061/(ASCE)CC.1943-5614.0000967.

[20] Shayanfar, J., Barros Joaquim, A. O. Design-Oriented Model of Unified Character to Determine Softening–Hardening Stress–Strain Behavior of FRP-Confined Concrete Columns of General Cross Section. Journal of Composites for Construction, 2024; 28: 04024059. doi:10.1061/JCCOF2.CCENG-4772.

[21] Wang, J., Xiao, H., Lu, L., Yang, J., Lu, S., Shayanfar, J. Axial stress-strain model for concrete in partially FRP wrapped reinforced concrete columns. Construction and Building Materials, 2024; 416: 135028. doi:10.1016/j.conbuildmat.2024.135028.

[22] Demir, U., Ispir, M., Sahinkaya, Y., Arslan, G., Ilki, A. Axial Behavior of Noncircular High-Performance Fiber-Reinforced Cementitious Composite Members Externally Jacketed by CFRP Sheets. Journal of Composites for Construction, 2019; 23: 04019022. doi:10.1061/(ASCE)CC.1943-5614.0000940.

[23] de Oliveira Diôgo, S., Raiz, V., Carrazedo, R. Experimental Study on Normal-Strength, High-Strength and Ultrahigh-Strength Concrete Confined by Carbon and Glass FRP Laminates. Journal of Composites for Construction, 2019; 23: 04018072. doi:10.1061/(ASCE)CC.1943-5614.0000912.

[24] Shayanfar, J., Barros, J. A. O., Rezazadeh, M. Generalized Analysis-oriented model of FRP confined concrete circular columns. Composite Structures, 2021; 270: 114026. doi:10.1016/j.compstruct.2021.114026.

[25] Shayanfar, J., Barros, J. A., Rezazadeh, M. Unified model for fully and partially FRP confined circular and square concrete columns subjected to axial compression. Engineering Structures, 2022; 251: 113355. doi:10.1016/j.engstruct.2021.113355.

[26] Shayanfar, J., Barros, J. A. O., Rezazadeh, M. Design-oriented stress–strain model for RC columns with dual FRP- steel confinement mechanism. Composite Structures, 2024; 330: 117821. doi:10.1016/j.compstruct.2023.117821.

[27] Vincent, T., Ozbakkaloglu, T. Influence of concrete strength and confinement method on axial compressive behavior of FRP confined high- and ultra high-strength concrete. Composites Part B: Engineering, 2013; 50: 413–428. doi:10.1016/j.compositesb.2013.02.017.

[28] Xiao, Q. G., Teng, J. G., Yu, T. Behavior and Modeling of Confined High-Strength Concrete. Journal of Composites for Construction, 2010; 14: 249–259. doi:10.1061/(ASCE)CC.1943-5614.0000070.

[29] Ozbakkaloglu, T. Axial Compressive Behavior of Square and Rectangular High-Strength Concrete-Filled FRP Tubes. Journal of Composites for Construction, 2013; 17: 151–161. doi:10.1061/(ASCE)CC.1943-5614.0000321.

[30] Wang, D. Y., Wang, Z. Y., Smith, S. T., Yu, T. Size effect on axial stress-strain behavior of CFRP-confined square concrete columns. Construction and Building Materials, 2016; 118: 116–126. doi:10.1016/j.conbuildmat.2016.04.158.

[31] Bengar, H. A., Kiadehi, M. A., Shayanfar, J., Nazari, M. Effective flexural rigidities for RC beams and columns with steel fiber. Steel and Composite Structures, 2020; 34: 453–465. doi:10.12989/scs.2020.34.3.453.

[32] Shayanfar, J., Rezazadeh, M., Barros Joaquim, A. Analytical Model to Predict Dilation Behavior of FRP Confined Circular Concrete Columns Subjected to Axial Compressive Loading. Journal of Composites for Construction, 2020; 24: 04020071. doi:10.1061/(ASCE)CC.1943-5614.0001087.

[33] Shayanfar, J., Barros, J. A. O., Rezazadeh, M. Stress–strain model for FRP confined heat-damaged concrete columns. Fire Safety Journal, 2023; 136: 103748. doi:10.1016/j.firesaf.2023.103748.

[34] Shayanfar, J., Akbarzadeh Bengar, H. Nonlinear analysis of RC frames considering shear behaviour of members under varying axial load. Bulletin of Earthquake Engineering, 2017; 15: 2055–2078. doi:10.1007/s10518-016-0060-z.

[35] Shayanfar, J., Bengar, H. A. Numerical model to simulate shear behaviour of RC joints and columns. Computers and Concrete, An International Journal, 2016; 18: 877–901. doi:10.12989/cac.2016.18.4.877.

[36] Han, Q., Yuan, W., Bai, Y., Du, X. Compressive behavior of large rupture strain (LRS) FRP-confined square concrete columns: experimental study and model evaluation. Materials and Structures, 2020; 53: 99. doi:10.1617/s11527-020-01534-4.

[37] Tariq, M., Khan, A., Shayanfar, J., Hanif, M. U., Ullah, A. A regression model for predicting the shear strength of RC knee joint subjected to opening and closing moment. Journal of Building Engineering, 2021; 41: 102727. doi:10.1016/j.jobe.2021.102727.

[38] Tariq, M., Khan, A., Ullah, A., Shayanfar, J., Niaz, M. Improved Shear Strength Prediction Model of Steel Fiber Reinforced Concrete Beams by Adopting Gene Expression Programming. Materials, 2022; 15: 3758. doi:10.3390/ma15113758.

[39] Shayanfar, J., Kafshgarkolaei, H. J., Barros, J. A. O., Rezazadeh, M. Unified strength model for FRP confined heat-damaged circular and square concrete columns. Composite Structures, 2023; 307: 116647. doi:10.1016/j.compstruct.2022.116647.

[40] Li, P.-D., Zeng, Q., Jiang, J.-F. Stiffness-based stress–strain model of FRP-confined high-strength and ultra-high strength concrete column with various corner radii. Construction and Building Materials, 2023; 409: 133873. doi:10.1016/j.conbuildmat.2023.133873.

[41] Jiang, T., Teng, J. G. Analysis-oriented stress–strain models for FRP–confined concrete. Engineering Structures, 2007; 29: 2968–2986. doi:10.1016/j.engstruct.2007.01.010.

[42] Lim, J. C., Ozbakkaloglu, T. Hoop strains in FRP-confined concrete columns: experimental observations. Materials and Structures, 2015; 48: 2839–2854. doi:10.1617/s11527-014-0358-8.

[43] Shayanfar, J., Akbarzadeh Bengar, H., Niroomandi, A. A proposed model for predicting nonlinear behavior of RC joints under seismic loads. Materials & Design, 2016; 95: 563–579. doi:10.1016/j.matdes.2016.01.098.

[44] Shayanfar, J., Bengar, H. A., Parvin, A. Analytical prediction of seismic behavior of RC joints and columns under varying axial load. Engineering Structures, 2018; 174: 792–813. doi:10.1016/j.engstruct.2018.07.103.

[45] Shayanfar, J., Hemmati, A., Bengar, H. A. A simplified numerical model to simulate RC beam–column joints collapse. Bulletin of Earthquake Engineering, 2019; 17: 803–844. doi:10.1007/s10518-018-0472-z.

[46] Guo, Y.-C., Xiao, S.-H., Luo, J.-W., Ye, Y.-Y., Zeng, J.-J. Confined Concrete in Fiber-Reinforced Polymer Partially Wrapped Square Columns: Axial Compressive Behavior and Strain Distributions by a Particle Image Velocimetry Sensing Technique. Sensors, 2018; 18: 4118. doi:10.3390/s18124118.

[47] Cao, Y.-G., Jiang, C., Wu, Y.-F. Cross-Sectional Unification on the Stress-Strain Model of Concrete Subjected to High Passive Confinement by Fiber-Reinforced Polymer. Polymers, 2016; 8: 186. doi:10.3390/polym8050186.

[48] Cao, Y., Liu, Y., Li, X., Wu, Y. Axial stress strain behavior of FRP-confined rectangular rubber concrete columns with different aspect ratio. Engineering Structures, 2023; 297: 116987. doi:10.1016/j.engstruct.2023.116987.

[49] Teng, J. G., Jiang, T., Lam, L., Luo, Y. Z. Refinement of a Design-Oriented Stress–Strain Model for FRP-Confined Concrete. Journal of Composites for Construction, 2009; 13: 269–278. doi:10.1061/(ASCE)CC.1943-5614.0000012.

[50] Wei, Y.-Y., Wu, Y.-F. Unified stress–strain model of concrete for FRP-confined columns. Construction and Building Materials, 2012; 26: 381–392. doi:10.1016/j.conbuildmat.2011.06.037.

[51] Fallah Pour, A., Ozbakkaloglu, T., Vincent, T. Simplified design-oriented axial stress-strain model for FRP-confined normal- and high-strength concrete. Engineering Structures, 2018; 175: 501–516. doi:10.1016/j.engstruct.2018.07.099.

[52] American Concrete Institute (ACI). ACI 440.2R-17: Guide for the design and construction of externally bonded FRP systems for strengthening concrete structures. Farmington Hills (MI): ACI; 2017.

[53] International Federation for Structural Concrete. CEB-FIP: Externally applied FRP reinforcement for concrete structures. Lausanne (CH): FIB BULLETIN NO. 90; 2019.

[54] Lim, J. C., Ozbakkaloglu, T. Stress–strain model for normal- and light-weight concretes under uniaxial and triaxial compression. Construction and Building Materials, 2014; 71: 492–509. doi:10.1016/j.conbuildmat.2014.08.050.

[55] Shayanfar, J. Integrated modelling strategy for FRP-based confinement imposed to RC columns: From undamaged to post-fire damage (PhD Thesis). Braga (PT): University of Minho; 2024.

[56] Akbarzadeh Bengar, H., Abdollahtabar, M., Shayanfar, J. Predicting the Ductility of RC Beams Using Nonlinear Regression and ANN. Iranian Journal of Science and Technology, Transactions of Civil Engineering, 2016; 40: 297–310. doi:10.1007/s40996-016-0033-0.

[57] Shayanfar, J., Omidalizadeh, M., Nematzadeh, M. Analysis-oriented model for seismic assessment of RC jacket retrofitted columns. Steel and Composite Structures, 2020; 37: 371–390. doi:10.12989/scs.2020.37.3.371.